

Dynamics of phase transitions at electrical explosion of wire

This article has been downloaded from IOPscience. Please scroll down to see the full text article.

1999 J. Phys.: Condens. Matter 11 2223

(<http://iopscience.iop.org/0953-8984/11/10/009>)

View [the table of contents for this issue](#), or go to the [journal homepage](#) for more

Download details:

IP Address: 171.66.16.214

The article was downloaded on 15/05/2010 at 07:11

Please note that [terms and conditions apply](#).

Dynamics of phase transitions at electrical explosion of wire

S I Tkachenko and N I Kuskova

Institute of Pulse Research and Engineering, National Academy of Sciences, pr. Oktyabrskii 43a, Nikolaev 327018, Ukraine

Received 30 June 1998

Abstract. Mathematical modelling of fast (microsecond) and superfast (nanosecond) regimes of electrical explosion of copper wires was carried out. The mechanism of electrical explosion was described as a process of propagation of the phase transition waves from outer boundary to the centre of the wire. The expressions for estimation of velocity of phase transition waves were obtained. Typical phase tracks were obtained for micro- and nanosecond electrical explosion of copper wires.

Metal–dielectric phase transition takes place without phase transition to a two-phase state in the skin in a nanosecond explosion. The process of propagation of the evaporation waves is the mechanism of wire electric explosion in the microsecond regime.

1. Introduction

There exists a number of technical and scientific aspects of application for electrical wire explosion. The great interest in the phenomenon is caused by the wide range of changeable parameters (temperature, density, pressure) and velocities of the processes.

Wire explosions are conditionally divided into fast and superfast; this is reasonable because of different mechanisms of wire destruction accompanying these explosions.

According to Bennett [1] the mechanism of electrical explosion development can be described as transformation of a liquid phase into a gaseous one, a so-called evaporation wave moving radially from the outer boundary to the centre of a wire. The method was further developed and used for the model of interaction of powerful laser radiation and condensed matter [2, 3]. In this model the size of the evaporation wave front is neglected, for the matter can be in two states: (1) conducting metal, not yet influenced by the evaporation wave; and (2) expanding nonconducting saturated steam [4]. This allows us to obtain approximate solutions for parameters of evaporated matter.

There exists also a kind of explosion characterized by low velocity of the fluid–gas phase boundary propagation and by a large size of the two-phase transitional layer [5]. In such case it is necessary to apply another model that takes into account processes in the transitional layer.

Evaporation is not a single phase transition that can take place at an electrical explosion. The influence of strong electric and magnetic fields on the conducting condensed matter during melting, evaporation etc can result in the following phase transitions: metal–semiconductor–dielectric. These phase transitions propagate like a wave [1, 5–7] under certain conditions.

In this work both fast and superfast explosions will be modelled; a model summarizing methods of describing these explosions is proposed. This model presents explosions as processes of generation and propagation of the above phase transition waves across the wire.

2. Theoretical model

Let us consider phase transition waves presenting a propagation process of strong local nonuniformity of electric and magnetic field if in this local region the mentioned phase transitions take place.

Change of any characteristic of matter f (specific internal energy ε , electrical conductivity σ and density ρ) is described by a continuity equation. At phase transition caused by current pulse Joule heating this equation can be written

$$\frac{\partial f}{\partial t} + v \frac{\partial f}{\partial r} = w \quad (1)$$

where v is the velocity of movement of matter, $w = w(j)$ is the rate of change of parameter f . Having designated the typical size of field nonuniformity by δ (in this region f changes abruptly from initial value f_0 to f^*) and coming to the coordinate system that moves with a velocity equal to the velocity of phase transition wave u and substituting $z = r + ut$ we obtain

$$(u + v) \frac{df}{dz} = w. \quad (2)$$

Since $|df/dz| \approx |\Delta f/\Delta z| = |f_0 - f^*|/\delta$, we can obtain an expression for an estimation of value of the propagation velocity of a phase transition

$$u \approx \frac{w\delta}{\Delta f} - v. \quad (3)$$

One or several characteristics of matter can change in the front of a single wave of phase transition.

One can see that there exists a threshold value of current density j^* at which a phase transition wave begins its propagation; j^* is defined from condition $u > 0$ i.e. $w(j^*)\delta/\Delta f - v > 0$. In case of nonexpanding wire ($v \equiv 0$) the right-hand side in equation (3) is always greater than zero, and therefore a phase transition wave begins its propagation from the outer boundary to the wire centre just when the temperature is equal to the temperature of phase transition.

A strong nonuniformity of current distribution takes place at superfast regimes of wire self-heating. The cause of this is generation and explosion of a skin. The wave movement is caused by displacement of current from the skin. This displacement takes place due to an abrupt decrease of electrical conductivity under heating of the metal wire by the high density current.

If the parameter f in equation (1) is the specific internal energy, then $w(j) = j^2/(\sigma\rho)$ is the rate of energy release determined by Joule heating. So expression (3) can be rewritten for estimation of the velocity of the so-called 'current wave'

$$u \approx \frac{j^2\delta_j}{\sigma\rho\Delta\varepsilon} \quad (4)$$

where $j = I/S$ is the current density; I is the heating current; $S = \pi(2a\delta_j - \delta_j^2)$ is the cross-sectional area of the skin for cylindrical wire; a is the wire radius; δ_j is the typical thickness of the skin; $\Delta\varepsilon$ is the change of specific internal energy of matter across the skin. The wave is displaced into a region of cool immovable metal, therefore $v = 0$.

At fast expansion of the wire melt layers a nonuniformity of magnetic field and current density can also arise. The diffusion equation for the magnetic induction B_φ can be written

$$\frac{\partial B_\varphi}{\partial t} + \frac{\partial(vB_\varphi)}{\partial r} = \frac{1}{\mu\sigma} \frac{\partial}{\partial r} \left(\frac{1}{r} \frac{\partial(rB_\varphi)}{\partial r} \right). \quad (5)$$

As one can see, an approximate solution of this equation for a magnetic field (taking into consideration the wire expansion and assuming that the wire is heated by the current pulse $I = I^0 e^{\omega t}$, where I^0 is the value of current in the melting moment) can be written as a power series expansion

$$B_\varphi = \frac{\mu I}{2\pi a^2} \sum_{n=0}^{\infty} b_{2n+1} r^{2n+1} \quad (6)$$

where $b_{2n} = 0$, $b_1 = 1$, $b_{2n+1} = [(\mu\sigma)^n / (2^{2n}(n+1)!n!)] \prod_{k=1}^n [2(k-1)\eta + \omega]$, $n \geq 1$; $\eta = v^{-1} dv/dt$; μ is the absolute magnetic permittivity.

Thus we can write

$$j = \frac{I}{\pi a^2} \left\{ 1 + \sum_{n=1}^{\infty} \left[\frac{1}{(n!)^2} \left(\frac{\sqrt{\mu\sigma\omega r}}{2} \right)^{2n} \prod_{k=1}^n \left(1 + \frac{2(k-1)\eta}{\omega} \right) \right] \right\}. \quad (7)$$

It follows from expression (7) that in slowly expanding wire ($\eta \ll \omega$) a skin is set up; its typical size can be estimated from the formula

$$\delta_j = 0.5(\mu\sigma\omega)^{-1/2} \quad (8)$$

under the condition

$$0.25\mu\sigma\omega a^2 \gg 1. \quad (9)$$

In the case of fast expanding wire another type of radial nonuniformity of current density can be set up. It is caused both by changing of the heating current and by changing of the wire radius. It is set up under the conditions

$$\eta \geq \omega \gg (0.25\mu\sigma a^2)^{-1}. \quad (10)$$

Its typical size δ_j is also determined by formula (8).

It follows from expression (9) that nonuniformity of current density is set up for $a = 10^{-4}$ m and $\sigma = 3 \times 10^6$ S m⁻¹ (these values correspond to a liquid copper wire) at $\omega > 10^7$ s⁻¹; its appearance is caused by fast changing of the heating current. In the fast expanding liquid copper wire ($\eta \sim \omega > 10^7$ s⁻¹) another type of nonuniformity of current density also arises.

Numerical experiments allow us to simulate regimes with both types of phase transition.

3. Numerical results for superfast regimes

Mathematical modelling of superfast regimes of a self-heating copper wire ($l = 15$ mm, $a = 0.1$ mm, where l is the wire length) with a current pulse was carried out. Diffusion and displacement of magnetic field was taken into account; it was assumed that the medium is weakly compressible because considerable development of hydrodynamic processes during $t \sim 10^{-8}$ s should not be expected; electrical conductivity was simulated by semiempirical expressions for solid and liquid copper [8], and by the model for the dense plasma state proposed in [9]; this model is based on interpolation formulas; the structure factor takes into account the change of particle interaction according to the density change with increasing of temperature; the effective approximation allows us to calculate an electron scattering on electrons, ions and neutrals; the method of calculation of a mean ion charge takes into account both thermal ionization and 'crushing' of an electron shell with pressure increase. It was assumed that conductivity vanishes at $\rho/\rho_0 \approx 0.15$.

Two different regimes of wire self-heating were investigated with the following circuit parameters: $C_1 = 20$ nF, $U_0 = 40$ kV, $L = 5$ nH (regime 2 differs from regime 1 by

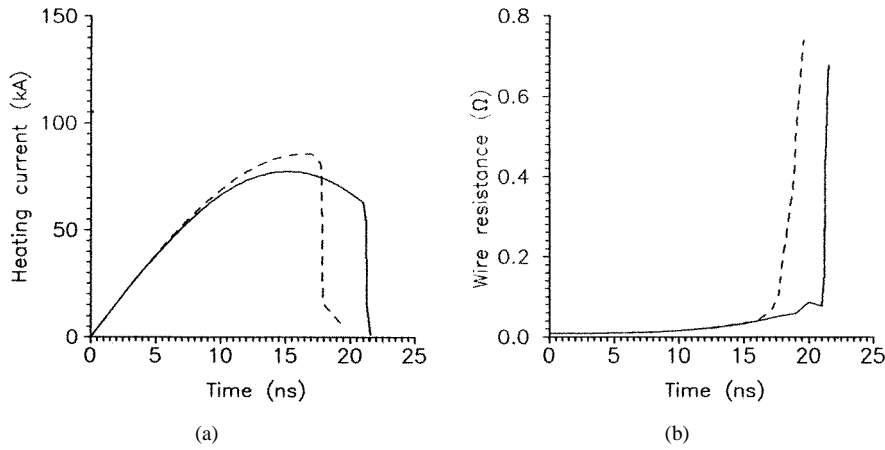


Figure 1. The time-dependent heating current (a) and wire resistance (b): broken curve (---), regime 2; solid curve (—), regime 1.

$C_2 = 25$ nF, where C is the capacity; U_0 is the initial voltage and L is the inductance). It was assumed that a copper wire was exposed to the open air. Figures 1–6 show the results obtained in these simulations.

Figure 1 shows the difference between regime 1 and regime 2 behaviour and illustrates in a general way the explosive phenomenon in terms of heating current (a) and wire resistance (b). One can see that abrupt decrease of heating current is set up simultaneously with abrupt increase of wire resistance and energy is released faster in regime 2 (the regime with greater stored energy).

Regime 1 has low energy because the stored energy ($0.5CU_0^2$) is less than is necessary for wire heating to temperatures up to the critical one and higher; at these temperatures a strong decrease of density takes place and metal–insulator phase transition is possible. Therefore such self-heating of wire proceeds like a melting phase transition wave. In this case the change of the internal energy of matter in the skin is equal to $\Delta\varepsilon = c\Delta T + \lambda$ (where c is the specific heat of solid metal; $\Delta T = T_m(P) - T_0$ is the temperature change at the melting wave front from the initial temperature to melting temperature $T_m(P)$, λ is the heat of melting). The electrical frequency for the regimes is $\omega = (LC)^{-0.5} \approx 10^8$ s $^{-1}$, therefore the skin size is $\delta_j \approx 1.5 \times 10^{-5}$ m. A strong nonuniformity of current distribution causes Joule heat release and matter melting in skin; this leads to an abrupt decrease of conductivity and to the current redistribution described by a diffusion equation. The typical time of current diffusion is $\tau_j = (\delta_j)^2/D$ (where $D = (\mu\sigma)^{-1}$ is the diffusion coefficient for the melt); in this case it is $\tau_j \approx 0.5$ ns.

Figure 2 shows the time dependent process of conductivity change against the radial distance at a series of times from the commencement of the simulation of regime 1. The maximum of conductivity corresponds to solid copper, and the minimum corresponds to liquid copper. The velocity of the melting wave obtained from the results shown in the figure is $u \approx 6 \times 10^3$ m s $^{-1}$. The same value can be obtained from equation (4) with j equal to the maximum value of current density.

Figure 3 shows the process of propagation of the current wave. The maximum of current density has a small increase as the conductivity of solid and liquid copper changes only by an order of magnitude. The peak value of current density is equal to $j \approx 1.3 \times 10^{13}$ A m $^{-2}$ on reaching the symmetry axis.

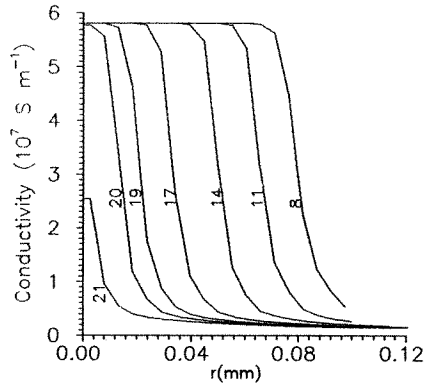


Figure 2. The change of conductivity against the radial distance for regime 1. Figures on the curves show the time in nanoseconds.

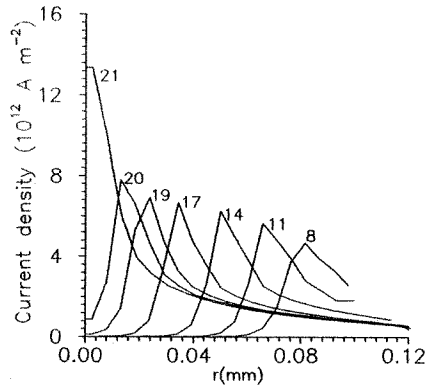


Figure 3. The change of current density against the radial distance. These curves illustrate the propagation of the melting wave across the wire section (regime 1). Figures on the curves show the time in nanoseconds.

Figures 4–6 show the change of conductivity and current density against the radial distance at a series of times from the commencement of the simulation of regime 2. The initial stage is the same as for regime 1: a melting wave is formed in the wire; the velocity of this wave is $u \cong 5 \times 10^4 \text{ m s}^{-1}$. Subsequent self-heating of melting part of the wire leads to fast expansion of the liquid metal ($\eta \cong 3 \times 10^8 \text{ s}^{-1}$ becomes comparable to ω). Therefore the second region of local nonuniformity of current density arises. Thus an abrupt decrease of density and conductivity in the new region of current nonuniformity causes formation of the second current wave by the time $t \cong 17 \text{ ns}$. In the wire front a liquid metal–dielectric phase transition occurs when density decreases to $\rho = 1.5 \times 10^3 \text{ kg m}^{-3}$. The second current wave has velocity $u \cong 10^5 \text{ m s}^{-1}$; it overtakes the first wave; after that they move together. The peak value of the second current wave becomes greater by an order of magnitude. Subsequently melting, transitions to plasma and to dielectric occur in the front of a single wave moving with velocity $u \cong 2 \times 10^4 \text{ m s}^{-1}$.

According to figure 1 an abrupt increase of wire resistance starts by the time $t \cong 17 \text{ ns}$; this corresponds to the time of the second current wave formation caused by the metal–dielectric transition.

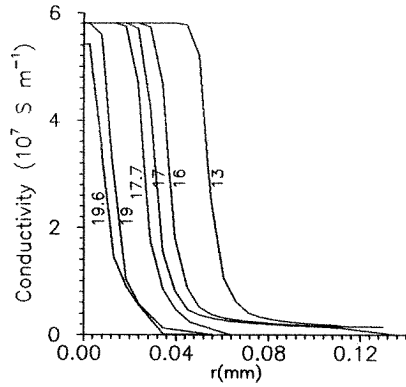


Figure 4. The change of conductivity against the radial distance for regime 2. Figures on the curves show the time in nanoseconds.

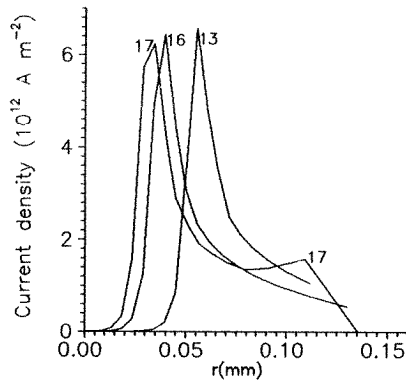


Figure 5. The change of current density against the radial distance. These curves demonstrate propagation of melting wave in a cross section and the rise of the second current wave (17 ns curve) in regime 2. Figures on the curves show the time in nanoseconds.

4. Mathematical modelling of microsecond regime

It is known that the initial stage of the fast regimes of wire self-heating are weakly nonuniform [5]; all parameters for a cylindrical wire are uniform along radial distance for solid and for liquid states except for magnetic pressure. Let us consider the development of boiling and evaporation processes in the wire uniformly heated with a current pulse; and let us find the typical size of the two-phase transitional layer.

It is known that temperature of boiling has a strong dependence on pressure, therefore a volumetric boiling is not possible even in case of quasi-uniform regimes of heating. Thus the propagation of a phase transition like a wave from the outside boundary to the centre of a wire is caused by pressure nonuniformity.

The boiling temperatures of the neighbouring layers of the wire differ from each other by the value $\Delta T_b \approx (dT_b/dP) \Delta P \approx |dT_b/dP| |dP/dr| \delta_p$ (where dP/dT_b is the pressure change against the boiling temperature along the curve of liquid–gas phase balance, r is the current coordinate of the wave front, δ_p is the size of the transition layer of the evaporation wave front). Magnetic pressure can be written as $P(r) = P(0)(1 - r^2/a^2)$ (where $P(0)$ is

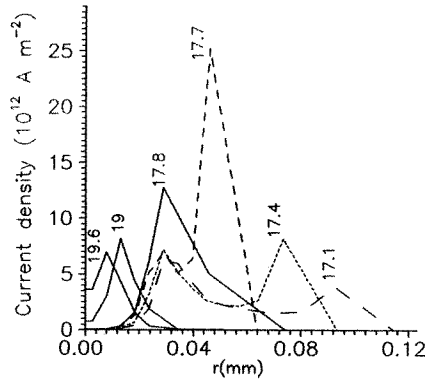


Figure 6. The change of current density against the radial distance. These curves demonstrate propagation of the first and second current waves in a cross section of wire (regime 2). Figures on the curves show the time in nanoseconds.

the pressure on the wire axis), then $|dP/dr| = P(0)(2r/a^2)$. Specific evaporation heats differ very little for neighbouring layers therefore continuous propagation of the evaporation wave is possible just at rising of the temperature of the next layer by ΔT_b during the evaporation time for the given layer. An equality $c_f \Delta T_b = \lambda_b$ is correct (where c_f is the specific heat of liquid metal; λ_b is the evaporation heat).

Thus the size of evaporation wave front for the considered case is determined by

$$\delta_p \approx \frac{\lambda_b}{c_f P(0)} \left| \frac{dP}{dT_b} \right| \frac{a^2}{2r}. \tag{11}$$

As the wire temperature is uniform up to the start point of boiling, the change of specific internal energy of the evaporation wave front is $\Delta \varepsilon = \lambda_b$, and the velocity of wave is determined by

$$u \approx \frac{j^2 \delta_p}{\sigma \rho \lambda_b} - v \tag{12}$$

where v is the velocity of heat expansion of liquid metal. In the case of the weakly nonuniform regime of wire self-heating expression (12) can be rewritten

$$u \approx \frac{I^2 R \delta_p}{m \lambda_b} - v \tag{13}$$

where m is the mass of the wire; $v \approx 0.5 \alpha r I^2 R / (m c_f)$ is determined as in [10], α is the expansion coefficient. The evaporation wave can move at $u > 0$; this is possible while the following inequality is realized:

$$\frac{a^2}{P(0) \alpha r^2} < \frac{dT_b}{dP}. \tag{14}$$

A mathematical simulation of a weakly nonuniform regime (regime 3) of self-heating of a copper wire ($l = 88$ mm, $a = 0.15$ mm) was carried out with the following circuit parameters: $C = 6 \mu\text{F}$, $U_0 = 20$ kV, $L = 5.4 \mu\text{H}$. It is assumed that the wire was submerged in water. A mathematical model and its finite-difference approximation had been described in [5, 11].

Figure 7 shows the time-dependent heating current (a) and wire resistance (b) for numerical and experimental data [12]. Figure 8 shows the radial distribution of conductivity at different moments of time. It demonstrates propagation of the evaporation wave front

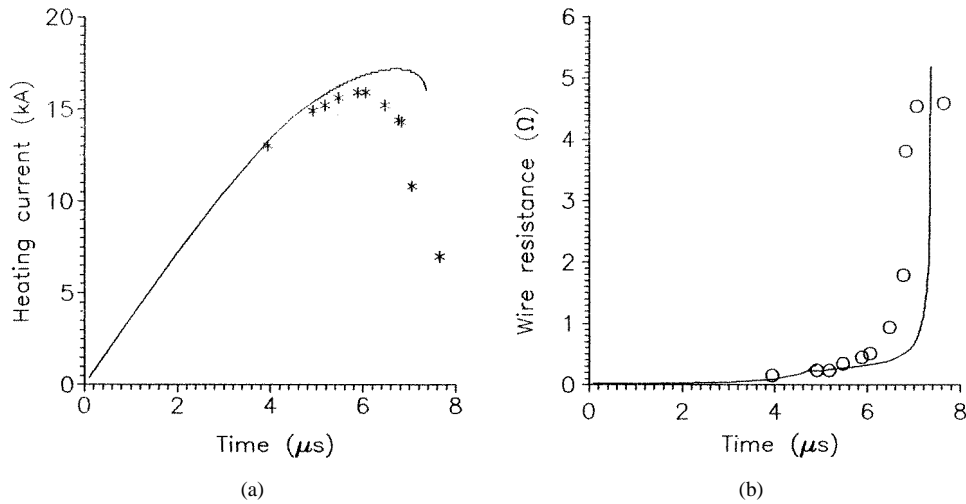


Figure 7. The time-dependent heating current (a) and wire resistance (b) for regime 3: —, numerical data; *, O, experimental data given in [12].

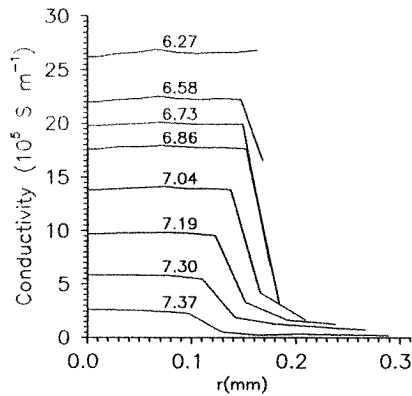


Figure 8. The change of conductivity against the radial distance for regime 3. Figures on the curves show the time in microseconds.

across the wire section. Obtained data allow us to estimate the velocity of the evaporation wave (its value $u \cong 70 \text{ m s}^{-1}$) and the size of its front ($\delta_p \cong 2.5 \times 10^{-5} \text{ m}$) thus one can see that the size of the two-phase transitional layer is great and can be up to $0.25a$). These values are in good agreement with values obtained from expressions (11) and (13).

It follows from experimental data [12] that an intensive evaporation of the wire layers begins at $t_s \approx 6.4 \mu\text{s}$ and the wire resistance rises up to $t_f \approx 8.4 \mu\text{s}$. These data allow us to estimate roughly the velocity of the evaporation wave according to expression $u_e \approx a/(t_f - t_s) \approx 75 \text{ m s}^{-1}$; this value is in accordance with those obtained from numerical data and from formulas (11) and (13).

It follows from the numerical results that the formation of the evaporation wave is considerably delayed as compared to the start of evaporation of the surface layer. This delay is caused by the fact that all parameters have the values when inequality (14) is not true up to the moment $t \cong 7 \mu\text{s}$.

Figure 9 shows a phase diagram of liquid copper for the second and third regimes. One can see that in the central layer magnetic pressure considerably exceeds critical pressure for both regimes; the same is true for the outer layer in regime 2; and the outer layer in regime 3 transits to the two-phase state early (before loss of layer conductivity).

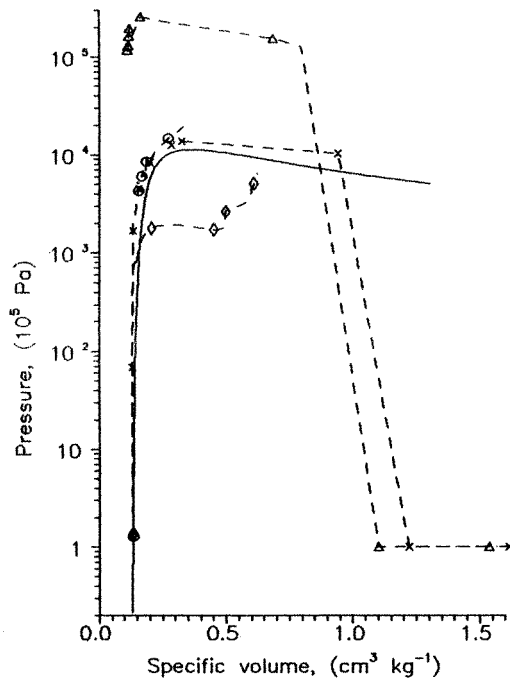


Figure 9. The phase diagram of liquid copper in the P - V plane. The solid curve bounds the liquid-vapour two-phase region. The broken lines (---) are the numerical tracks for regimes 2 and 3. The data points (\circ , \diamond) are those of regime 3 and (Δ , \times) are those of regime 2 obtained for central and outer layers, respectively.

In the nanosecond regime (regime 2) a liquid metal–dielectric phase transition occurs in the front of a single wave. Its propagation is caused by displacement of current from the layer in which the above phase transition takes place; thus up to loss of conductivity a phase transition to a two-phase state does not happen; therefore the velocity of this phase transition wave can exceed the sound velocity. It results from numerical modelling that the phase transition to a two-phase state of any layer takes place just after the loss of layer conductivity in nanosecond regimes.

In the microsecond regime (regime 3) magnetic pressure in the central layer exceeds the copper critical pressure, therefore it does not vaporize up to $7.4 \mu\text{s}$. A large part of the wire loses its conductivity due to propagation of the boiling wave but the central part loses its conductivity due to propagation of the metal–dielectric phase transition wave. The presence of two powder fractions (these fractions considerably differ from each other) in the products of conductor dispersion proves this. In [13] was reported that although the main part of particles have typical size $\sim 20 \text{ nm}$, during explosion another type of particle was registered according to light scattering at the stage of abrupt rise of wire resistance; their size was reported to be about 100 nm .

5. Conclusions

The theoretical and numerical modelling of micro- and nanosecond explosions of wire were carried out; this allows us to show the dynamics of different phase transitions. The conditions needed for formation and propagation of phase transition waves were investigated. Theoretical and numerical data are in accordance with experimental data.

The process of propagation of the phase transition waves is the mechanism of wire electric explosion. This leads to a change of phase state of matter, its electrical and thermodynamical properties and first of all to an abrupt decrease of density and conductivity, and at a certain regime conductivity entirely vanishes.

The formation of phase transition waves takes place due to nonuniformity of any parameter of the wire matter caused by the influence of strong pulsed current. The velocities of phase transition waves can differ from each other by several orders of magnitude. The start of propagation of a wave is characterized by an abrupt increase of wire resistance due to the metal–dielectric transition in its front.

References

- [1] Bennett F D 1965 *Phys. Fluids*. **8** 1425
- [2] Knight Ch J 1979 *AIAA J.* **17** 519
- [3] Breslavskii P V, Mazhukin V I and Samohin A A 1991 *Doct. Akad. Nauk SSSR* **320** 1088
- [4] Bennett F D 1971 *Physics of High Energy Density, Proc. Int. School Phys. 'Enrico Fermi'* ed P Caldirola (New York: Academic)
- [5] Kuskova N I, Tkachenko S I and Koval S V 1997 *J. Phys.: Condens. Matter* **9** 6175
- [6] Burtzev V A, Kalinin N V and Luchinskii A V 1990 *Electrical Explosion of Conduction and its Application in Electrophysical Equipment* (Moscow: Energoatomizdat)
- [7] Kolgatin S N, Polishchuk A Ya and Shneerson G A 1993 *Teplofiz. Vys. Temp.* **31** 890
- [8] Knoepfel H 1970 *Pulsed High Magnetic Fields* (Amsterdam: North-Holland)
- [9] Ebelin W, Fortov V E, Gryaznov V K, Forster A and Polishchuk A Ya 1990 *Thermophysical Properties of Hot Dense Matter* (Leipzig: Teubner)
- [10] Kuskova N I and Tkachenko S I 1996 *Pis. Zh. Tekh. Fiz.* **22** 30
- [11] Tkachenko S I 1995 *Matem. Modelirov.* **7** 3
- [12] Koval S V, Kuskova N I and Tkachenko S I 1996 *Preprint IPRE Natl. Acad. Sci. of Ukraine* **27**
- [13] Weber F N and Shear P P 1969 *J. Appl. Phys.* **40** 3854